Version 8, mise à jour 22/06/2023

Christian BARON, Mathieu CASTETS, Jérémy LAVARENNE

English translation : Stanley ORAMAH, U. Coventry

Photo : Elodie Vintrou (thèse Cirad)

SARRA-O:

A tool for analyzing the Resilience of Agriculture to Climate Risks

User Manual

Contact : sarra-h@cirad.fr / https://sarra-h.teledetection.fr

Keywords : Spatialise Crop model, Early warning system, climate services, yield prediction

1. General Presentation

SARRA-O embodies a spatialized translation of SARRA-H, a crop simulation model at the scale of cultivated plots. By integrating simple equations to simulate key processes, SARRA-H provides a representation of plant growth dynamics, particularly in environments subjected to water stress. SARRA-H has been calibrated and validated through controlled experiments on various species and varieties (millet, maize, sorghum, rice, soybeans) and in different agro-climatic regions, notably in Africa. Furthermore, it has been validated in peasant environments through surveys and field measurements (Kouressy et al., 2007; Traoré et al., 2011; AMMA, SIGMA projects…).

SARRA-O inherits the simulation capabilities of SARRA-H and transposes them through a new computer development environment, the Ocelet modeling platform (Degenne and Lo Seen, 2016; Degenne et al., 2009), which optimizes and automates the management of large sets of spatialized data, such as time series of raster images and raster or vector thematic maps underlying calculations. Thus, SARRA-O refers to both the software and the underlying model, distinguishing itself by its ability to process data at various spatial and temporal scales.

Since the late 2000s, the spectacular evolution of satellites and satellite data processing has led to improved dissemination and increased accessibility to spatialized meteorological and climatic data, such as rainfall estimates (RFE), temperature, and global radiation. These data, available to all, have spatial (from meters to kilometers) and temporal (from intra-daily to decadal) resolutions adequate for effectively simulating plant growth and monitoring crop conditions throughout the seasons.

Moreover, these data can be provided in near real-time through certain systems, with processing and dissemination delays ranging from a day to a few days, depending on processing modalities. They constitute the input data for SARRA-O, and their quasi-instantaneous access, combined with their homogeneity over vast territories, is essential for enabling homogeneous large-scale simulations. This feature is fundamental for applications such as continuous monitoring of crop conditions during the agricultural season and the establishment of early warning systems (EWS).

The SARRA-H&O models simulate three main processes: 1) the water balance, 2) the carbon balance, 3) the evolution of plant phenological phases including photoperiodism. They use input data such as rainfall (mm), minimum and maximum temperatures (°C), global radiation (J/m²/d), and evapotranspirative demand (mm).

Furthermore, the processes integrated into these models take into account the main aspects of agricultural practices: the properties specific to different cultivars, sowing strategies (including simulating sowing dates), overall technical level and fertilization, as well as irrigation strategies (including simulation of irrigation scenarios).

This set of features has led to a wide range of impact studies and risk analyses. These, ranging from the plot scale to the regional scale, address various themes: climatic variability, climate change, different agricultural strategies adopted by farmers, adaptation of cultivars to their environment, and the deployment of early warning systems (EWS). Thus, these models prove to be valuable tools for contemporary agriculture, which must face major climatic and environmental challenges.

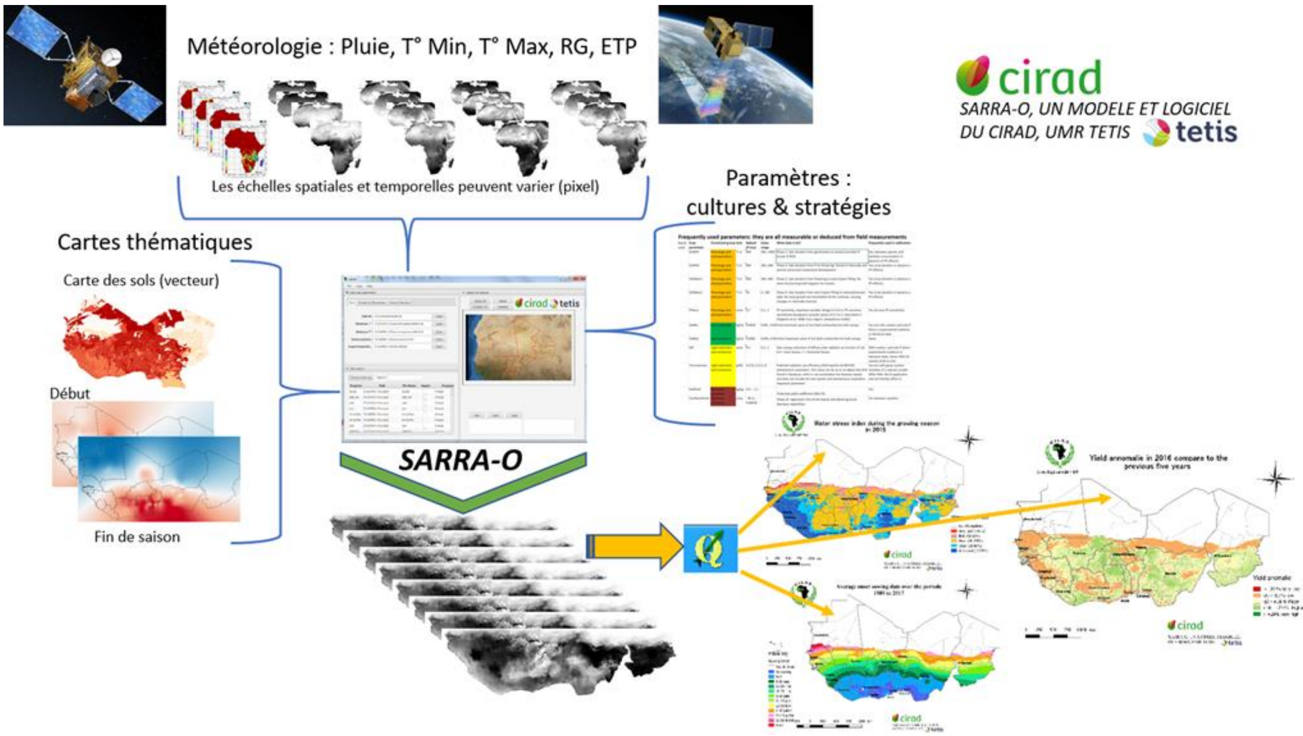

1.1. Objectives, Constraints, and Environments

The interface of the SARRA-O software is specifically designed to facilitate its use in the provision of climate services during the agricultural campaign and for its implementation within an early warning system (EWS) for food security. This design has been guided by several key criteria for evaluating crop yield and production forecasting, as described by the FAO ("Crop Yield Forecasting: Methodological and Institutional Aspects", 2016): semi-real-time; predictive capacity of the model and sensitivity to extreme events; simplicity of model structure and required data.

An important constraint for semi-real-time simulation in the EWS is the need to collect data on precipitation, temperature, global radiation, and potential evapotranspiration (ETP) from a sufficiently dense and well-distributed network of ground stations. This is particularly challenging when this network mainly consists of non-connected, manual, or automatic stations. This centralization process is time-consuming and often suffers from significant random data gaps. In response, and within the context of West Africa, AGRHYMET as well as several meteorological centers have equipped themselves with a satellite link to receive semi-real-time estimates of daily precipitation derived from the Météosat satellite: TAMSAT (Maidment et al., 2016), with a spatial resolution of 3.7 km and a daily time step. Other meteorological data required for the model were also available in semi-real-time at a spatial resolution of 16 km and a time step of 10 days (ECMWF ERA-interim (Berrisford et al., 2011)).

Based on the accessibility of this data, and drawing on extensive experience and partnerships in various tropical countries, notably in Africa, the SARRA-O interface has been developed and adapted in partnership with AGRHYMET according to needs, requests, and feedback. Since 2016, the software has been tested, improved, and most importantly, used in real campaign monitoring situations within the EWS developed by AGRHYMET.

The SARRA-O platform allows for managing these different spatial and temporal resolutions to conduct simulations in selected territories, countries, or regions. The model can also handle many other sources of climatic data derived from satellite data or climate models.

The user interface has been developed considering various levels of analysis and services, at the regional level and at the administrative and/or national level. For the EWS developed by AGRHYMET, an initial level of analysis and dissemination is carried out for the entire region (ECOWAS). Moreover, multidisciplinary national working groups have been established in the member countries of CILSS to work closely with AGRHYMET to disseminate more specific country information.

The quality of a model is also determined by its level of performance and its usage environment. For these reasons, simulations of models at the regional and/or national scale for an entire season must be achievable within a reasonable timeframe using a standard desktop or laptop computer. For example, a simulation of an entire year over the ECOWAS and CILSS countries (600,000 pixels) varies from 7 to 15 minutes depending on the computer. These performances are significant when one wishes to study a range of contrasting situations, test the relevance of the model outputs, or of the implemented system and services offered.

1.2. The SARRA-O Spatialized Crop Model

A spatially explicit crop model, like SARRA-O, is capable of conducting crop simulations over a large area and accounting for a variety of different environmental situations within that region. In this type of model, input and output data are often presented in the form of vector maps or raster images. Vector maps may include information such as soil types and aggregated potential yield at the administrative level. Raster images may include estimates of satellite-derived precipitation, maps of water stress indices, and information on crop yields.

SARRA-O, the spatialized crop model presented here, retains the same crop processes as its predecessor SARRA-H, simulating processes at the plot scale:

- The water balance considers plant water needs and available soil water, allowing estimation of actual plant transpiration compared to their demand. The soil is divided into two compartments, a surface layer of 20 cm to calculate evaporation and a deeper layer to the wetting front.
- The carbon balance simulates radiation interception by leaves and the conversion of this energy into biomass, which is then distributed into various plant compartments (root, leaf, stem, and grains) and also consumed by the plant's maintenance respiration process.
- Plant phenology is simulated in several phases: emergence, vegetative phase, reproductive phase, grain filling phase, and desiccation phase. The duration of these phases is simulated based on the average daily temperature (degree days). In some cases, for photoperiodic cultivars of millet or sorghum, a photoperiodic phase is inserted between the vegetative and reproductive phases, which is linked to the length of the day (long or short).

The spatialized crop model SARRA-O simulates biomass production, which is limited by water resources and solar radiation. To do this, it uses climatic data such as precipitation, temperature, global radiation, and evapotranspiration. Additionally, it takes into account several important aspects of agricultural practices, including sowing strategies (such as sowing date and density), irrigation strategies (including water volumes and irrigation schedules), choice of cultivated varieties, and overall level of intensification.

To more efficiently model the variety of agricultural practices in a given territory, and due to the difficulties in obtaining detailed information on these practices, the model defines overall levels of intensification that encompass various situations and constraints. These levels take into account factors such that quality of seeds, soil tillage, weed management, and fertility level (both natural soil fertility and due to fertilizer inputs). Four levels of intensification have been defined, reflecting situations ranging from "very poor" (I1) to "very good" (I4). These levels have a direct influence on the amount of biomass produced each day and, ultimately, on the achievable yield of the crop. In other words, the level of intensification is a determining factor in agricultural production, according to SARRA-O simulations.

1.3. The SARRA-O Software

The SARRA-O software is a versatile platform that has been designed to be both powerful and user-friendly. It is accessible to a wide range of users, including those without specialization in agronomy, agriculture, geomatics, or climatology. To use this software, one simply needs to understand how to choose simulation options based on the expected results for the analysis objectives or services that the user wishes to obtain or disseminate. It is compatible with various operating systems, such as Windows, Unix/Linux, and Mac, making it easy to use on a standard desktop computer. In terms of performance, a simple desktop computer is sufficient: a year of simulations takes only a few minutes for a country, and from 7 to 15 minutes, depending on the computer, for almost all of West Africa, defined here by 600,000 pixels (i.e., 600,000 annual simulations).

SARRA-O stands out for its ability to manage complex spatial and temporal data, as well as its ability to scale. It generates outputs in the form of maps (raster files in TIF format) and/or text files, which are easy to process, particularly by open-source software. It also automatically manages various sources of input data, whether they are text files, raster or vector maps. These data can include soil characteristics, plant characteristics, as well as thematic maps and/or time series from satellite data. The fundamental principles that have guided the development of the different versions of the SARRA model are simplicity, robustness, and performance. The user interface has been developed with a particular focus on ease of use and a didactic approach.

The SARRA crop model has been developed and tested in quasi-operational conditions within the Ocelet Modeling Platform (OMP). For daily use, we have developed a simple and customized user interface that allows users to easily produce a wide range of predefined simulations. This interface, developed in Java, connects to an executable file (.jar) containing SARRA-O. It consists of four panels to manage: i) the simulation study area, ii) simulation scenarios, iii) output variables, and iv) launching simulations with a window indicating the progress of simulations. A brief overview is provided here, but it will be further detailed in the next chapter.

Simulation Study Area: In this example, the default study area corresponds to simulations conducted at AGRHYMET covering the 17 countries of the CILSS/ECOWAS region. The same software is also available for each of the ECOWAS countries, or any other country, to conduct simulations within their country and/or administrative regions.

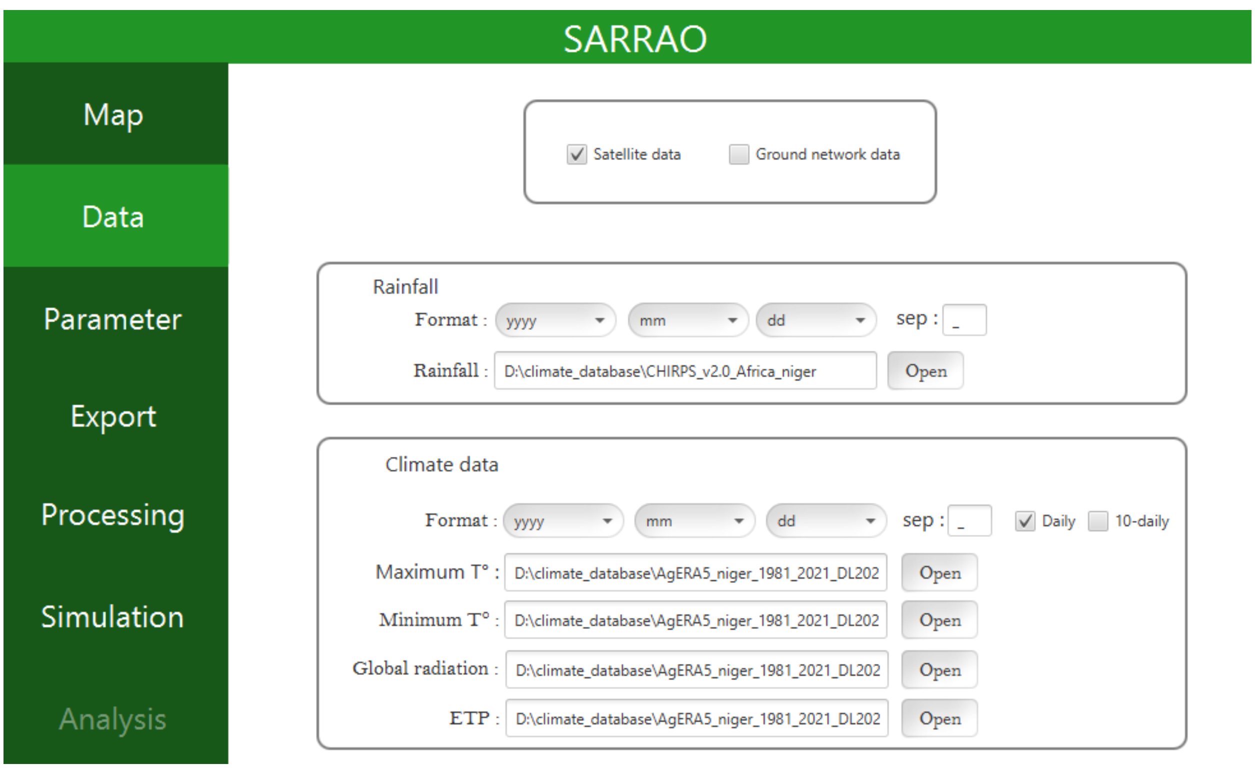

Meteorological Input Data: The chronological series of precipitation estimates, temperature, global radiation, and evapotranspiration are in the form of raster images stored in separate directories accessible to the model. The raster images are in GeoTIFF format (.tiff) with pixels coded in real values respecting the following units: mm (rainfall), °C (Temperature), kJ/m²/day (Global Radiation), and mm (Evapotranspiration). Precipitation images are read at each daily time step, while other meteorological data are read every ten days.

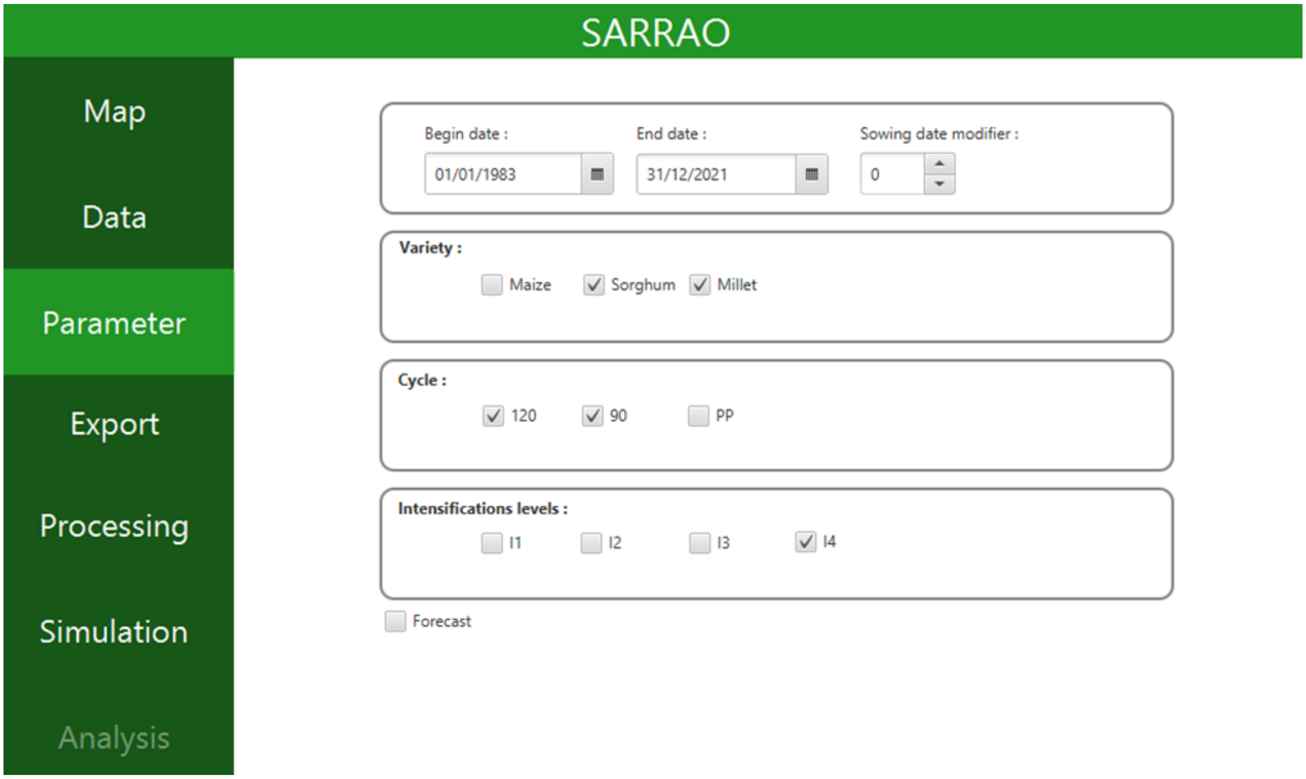

Simulation Parameters:

Start and end of simulations,

Planting strategy,

Simulation period.

Selected Varieties:

This initial version of the interface allows simulating typical varieties of three species (millet, sorghum, and maize), with two cycle lengths (90 and 120 days), photoperiodism according to the cultivar, and 4 overall levels of intensification (I1 to I4).

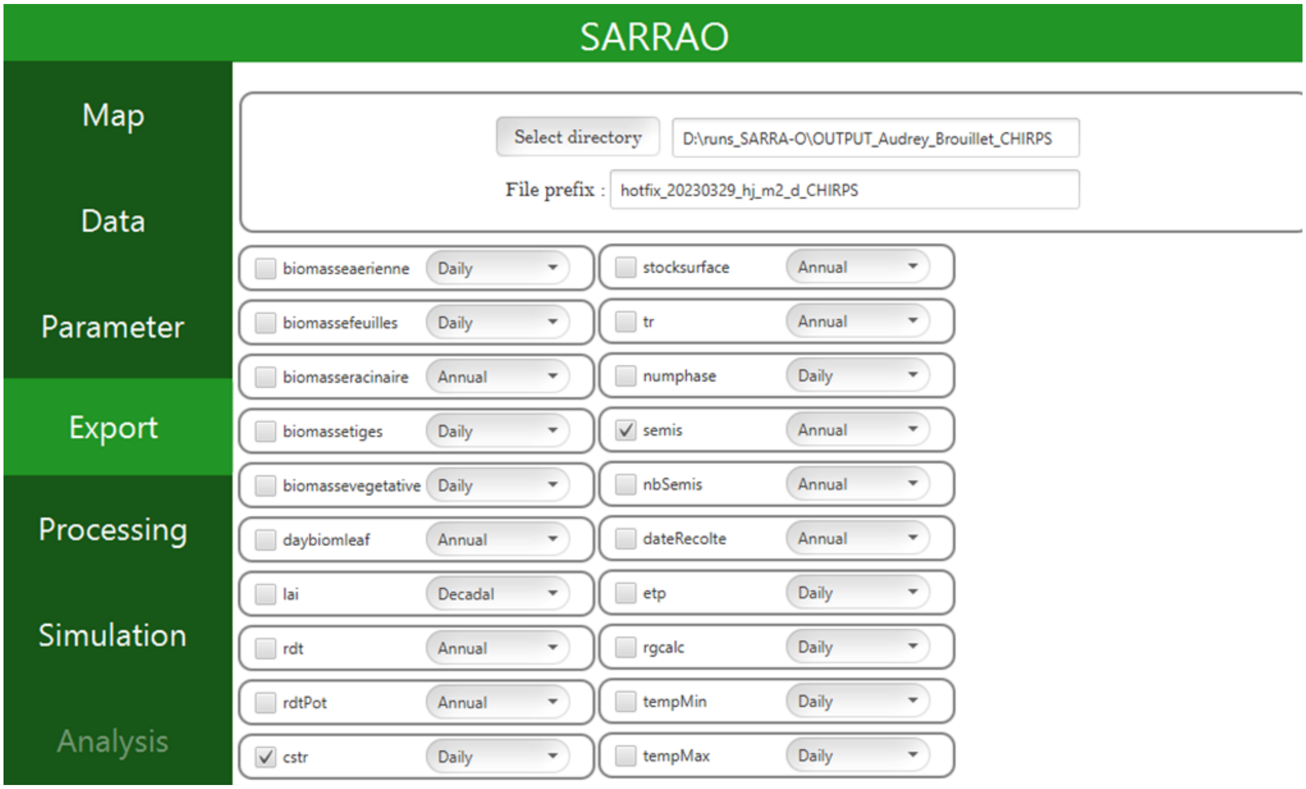

Output Variables:

Each of these variables can be tracked at different frequencies (daily, weekly, monthly) and saved as GeoTIFF images in the selected directory. These layers of information can then be used to generate maps of indices (such as crop water satisfaction index) or yield anomalies. These maps, easily and quickly produced, allow for rapid dissemination, such as in the monthly bulletins of AGRHYMET. For their cartographic formatting, we recommend the use of a free and open-source software, QGIS (Quantum GIS), for which we offer, during training sessions, a quick introduction as well as a series of legends, logos... tailored to the outputs provided by the software...

Main input parameters of the model:

Main Input Parameters of the Model:

Type of Data	Format	Resolution	Source	Time Step
Country	Shape	NA	NA	NA
Soil Type	Raster	3.7 km	FAO	NA
Start of the Season	Raster	3.7 km	AGRHYMET	NA
End of the Season	Raster	3.7 km	AGRHYMET	NA
Precipitation	Raster	3.7 km	TAMSAT	Daily
Minimum Temperature	Raster	28 km	ECMWF	10 days
Maximum Temperature	Raster	28 km	ECMWF	10 days
Potential Evapotranspiration	Raster	28 km	ECMWF	10 days
Global Radiation	Raster	28 km	ECMWF	10 days

Note: Table 1: 1989-present

Global Data Management

The SARRA-O software utilizes free and openly accessible data.

2.1. "Data" Tab: Climate Data and Parameters

For each type of climate data, you can define the access directory. The files must be provided in GeoTIFF format, with one file corresponding to one day or one decade. SARRA-O identifies the date from the file name, and it is necessary to specify the date format in the file name, as well as the date separator used. Rainfall data must be daily, while it is possible to work with decade-long data for climate. In the latter case, care must be taken to verify whether the data included in the decade files are cumulative or averages over the ten days.

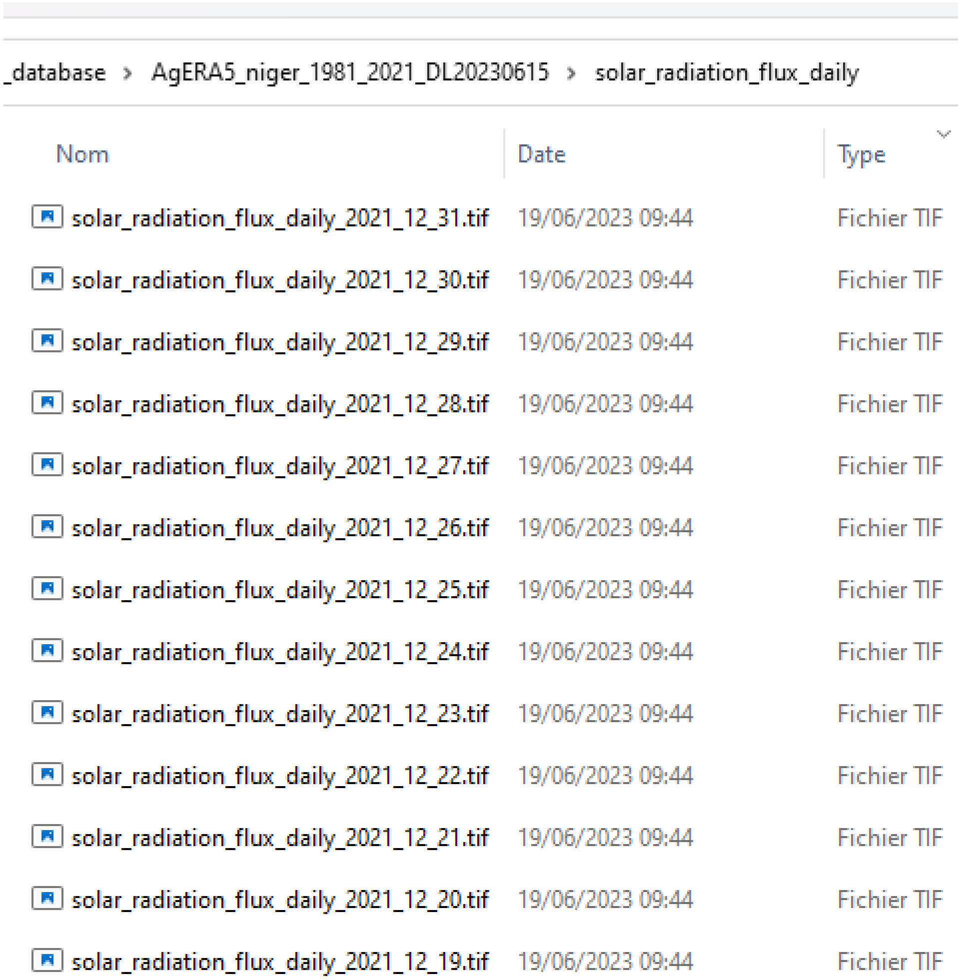
_database > AgERA5_niger_1981_2021_DL20230615 > solar_radiation_flux_daily
Nom
Date
Type
solar_radiation_flux_daily_2021_12_31.tif 19/06/2023 09:44 Fichier TIF
solar_radiation_flux_daily_2021_12_30.tif 19/06/2023 09:44 Fichier TIF
solar_radiation_flux_daily_2021_12_29.tif 19/06/2023 09:44 Fichier TIF
solar_radiation_flux_daily_2021_12_28.tif 19/06/2023 09:44 Fichier TIF
solar_radiation_flux_daily_2021_12_27.tif 19/06/2023 09:44 Fichier TIF
solar_radiation_flux_daily_2021_12_26.tif 19/06/2023 09:44 Fichier TIF
solar_radiation_flux_daily_2021_12_25.tif 19/06/2023 09:44 Fichier TIF
solar_radiation_flux_daily_2021_12_24.tif 19/06/2023 09:44 Fichier TIF
solar_radiation_flux_daily_2021_12_23.tif 19/06/2023 09:44 Fichier TIF
solar_radiation_flux_daily_2021_12_22.tif 19/06/2023 09:44 Fichier TIF
solar_radiation_flux_daily_2021_12_21.tif 19/06/2023 09:44 Fichier TIF
solar_radiation_flux_daily_2021_12_20.tif 19/06/2023 09:44 Fichier TIF
solar_radiation_flux_daily_2021_12_19.tif 19/06/2023 09:44 Fichier TIF

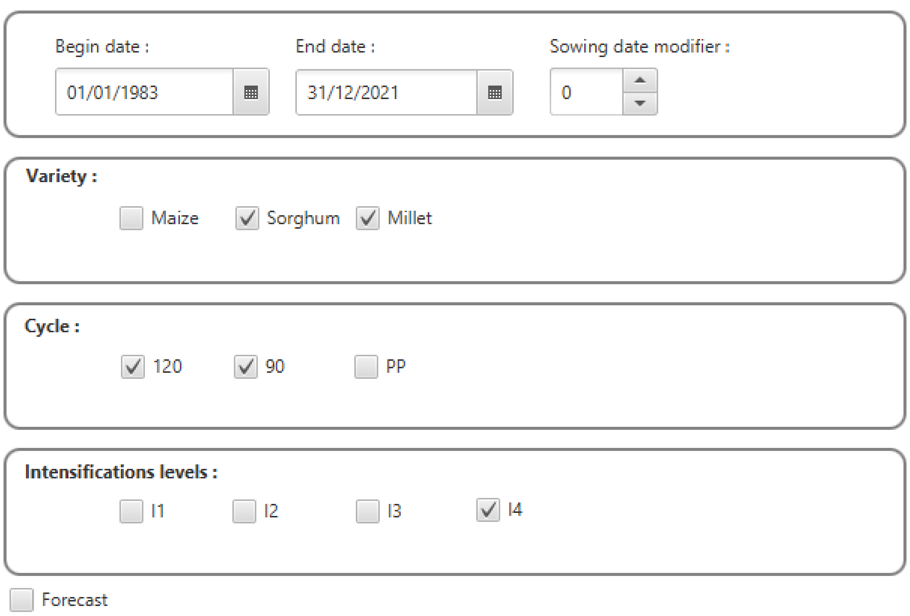
Begin date :
01/01/1983
End date :
31/12/2021
Sowing date modifier :
0
Variety :
Maize
Sorghum
Millet
Cycle :
120
90
PP
Intensifications levels :
I1
I2
I3
I4
Forecast

2.2. "Parameter" Tab: Simulation Parameters

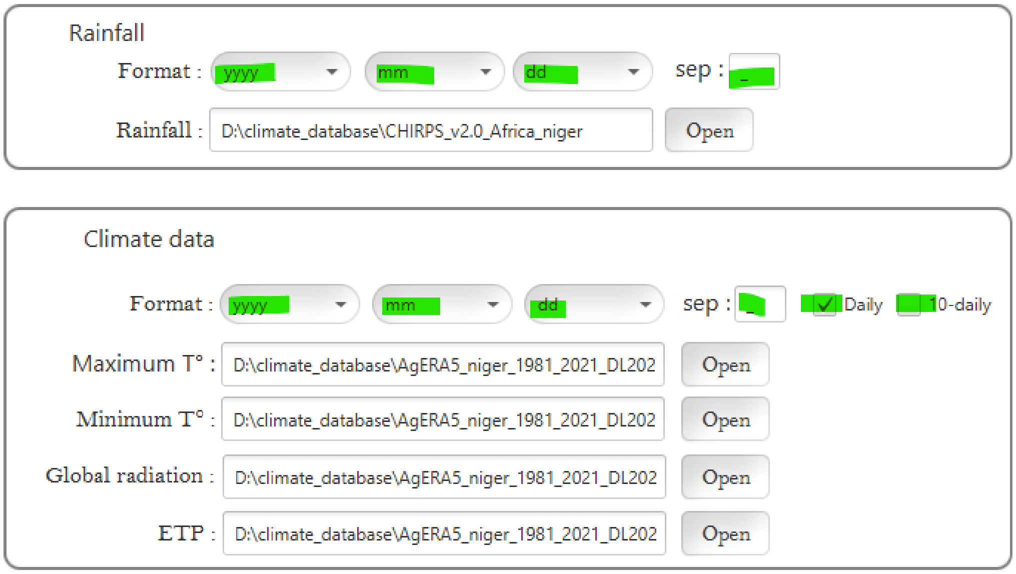

In the "Simulation Parameters" screenshot below, you define the start and end dates of the simulations as well as the offset in days based on the average planting date, reported for each pixel (with a resolution of 3.7 km in the case of TAMSAT) from the map of average planting dates calculated by AGRHYMET (p. 20). Depending on the available data, real-time planting time during ongoing campaign monitoring can define the end of the simulations: for example, on 01/08/2016. Outside of campaign monitoring, you can also conduct multi-year analyses or analyses for a particular year: for example, for a series of years (from 01/03/2007 to 30/11/2015), the simulation will be conducted for each year from 01/03 to 30/11, otherwise for a particular year, you specify the same year at the start and end of the simulations. Finally, the search for the planting date is conditioned by the defined delay around the average planting date. This option is detailed in the Diagnostic chapter -> Planting Date (p. 17). Similarly, the forecast option (button "Forecast") will be detailed in the Forecast chapter (p. 20).

2.3. "Map" Tab: Definition of the Geographic Area for Simulations

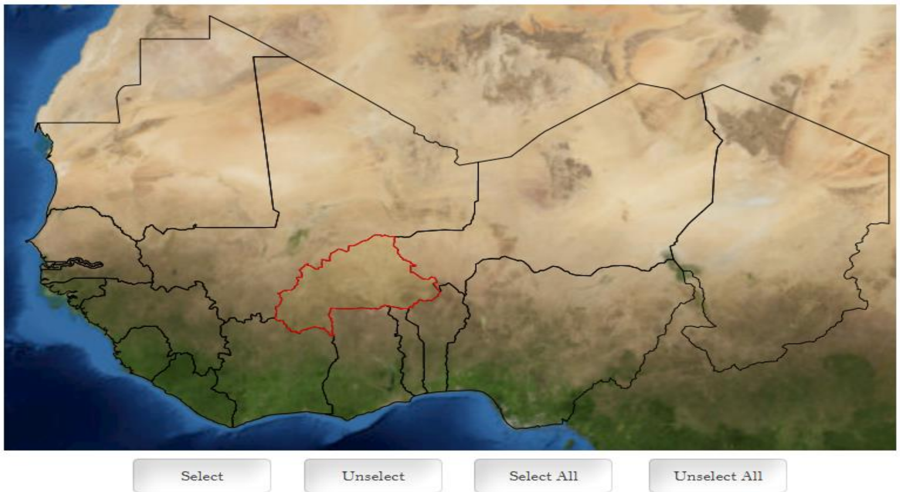

2.3. "Map" Tab: Definition of the Geographic Area for Simulations

The definition of the geographic area is tailored to each country and desired administrative division, and can be adapted to other territories (e.g., Mozambique at the end of the document). In the example presented, only Burkina Faso has been selected. You can simulate over the entire proposed geographic area (default choice) or choose one or more subsets (here, administrative subsets). To do this, you deselect everything: "Unselect All," then click on the "Select" button and choose one or more subsets by clicking on this set. It should be noted that for simulations to launch and be conducted correctly, the extent of rainfall and climate data must be larger than the extent of the selected country or countries.

2.4. "Export" Tab: Definition of the Simulated Output Variables

If desired, you can define different directories based on sets of simulations you perform with the "Choose directory" button. After selecting the directory, it is automatically assigned to the entire list of output variables. In the example presented, the data will all be exported to the OUTPUT_... folder. A folder will be created for each variable for which export has been requested (cstr and semis), and within this folder, the name of each file will contain the hotfix_xxx prefix. For the cstr variable, one GeoTIFF file will be exported per day, while for the semis variable, only one file will be exported per simulated season, so here at the end of the season.

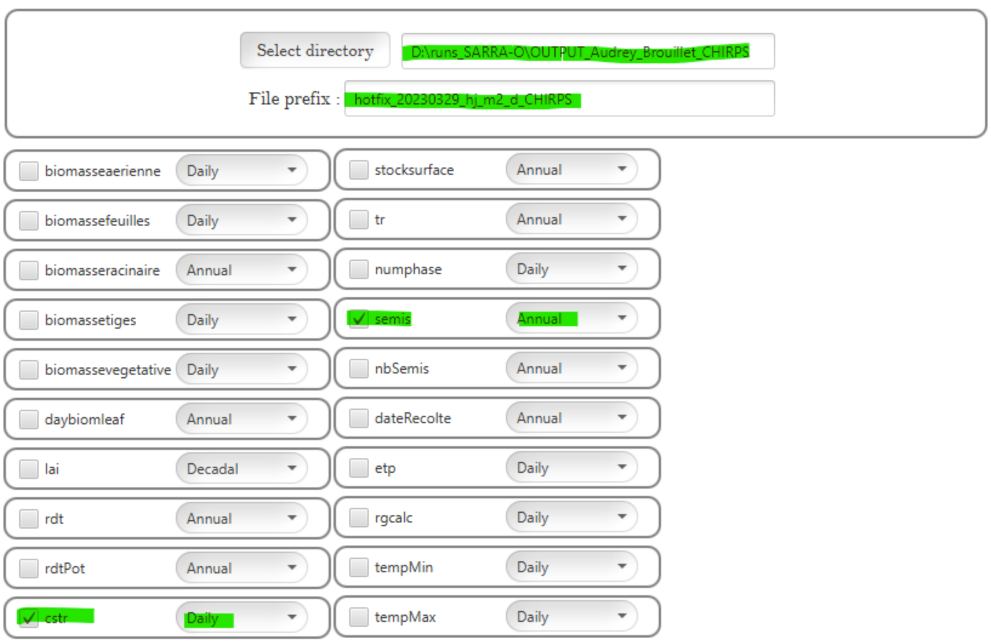

To select or deselect a variable, simply click on the "Export" box next to the variable. If it is checked, the variable is selected; if it is empty, it is not selected. You can choose a list of different output variables (raster images). Additionally, you can also choose the time step for these output variables under the "Frequency" column by clicking on the displayed frequency (here, by default, "Annual"). A dropdown menu allows you to choose different time steps (from daily to annual).

In the example above, three output variables have been selected. The file names are constructed based on the different options chosen:

- rdtMais_90_F4_2016.tif: This means that the variable rdt, which represents yield at harvest, has been chosen. It concerns a short-cycle maize of 90 days (Mais_90), with a very good intensity level (_F4), and the simulation year is 2016. Finally, the file format is a .tif format, which is a standard recognized by many georeferenced data processing software.

Thus, for the choice of the output variable rdtPot, which represents yield at flowering, we would have: rdtPotMais_90_F4_2016.tif In the case of sub-annual output, the date is specified with the number of the decade in the month (year_month_DecadeNumber) or the date of the day if it is daily output (year_month_day). For example, 2016_01_01 for the first decade of January 2016 or January 1, 2016 for daily output.

2.5. Launching and Saving Simulation Scenarios

When switching to the "simulation" tab, the software may slow down a bit because it works in the background to prepare files for simulation. If the period is long, it is normal for this step to take a few tens of seconds. Launching a simulation scenario is as simple as pressing a button: "Run"! The parameters used during the previous run are automatically saved in memory, so you can relaunch a simulation exactly as it was before. You can tell if there are no issues when the message "Running" is displayed, the simulation parameters are recalled, and the day count is running. If there are no additional messages, and/or the day count is not running, there may be an issue with the data. Similarly, if the simulation stops on a given day, you will need to check that the data file for that day has not been corrupted during download. It is advisable, if the simulations do not run smoothly, to double-check the directories for your input data: the dates and years, as well as the presence of file series corresponding to the defined periods.

3. The various use cases of SARRA-O

SARRA-O is generally used in three different modes. The first, called diagnostic mode, is routine use, in semi-real time, to monitor the growing season and quickly detect anomaly areas. The second, called forecast mode, involves generating, in the middle of the growing season, an assessment of the potential yield at harvest, as well as an associated probability of yields at the end of the season using historical series, or estimating this end-of-season yield using seasonal forecasts from meteorological models. These two modes are managed from the user interface. A third mode, called analysis and improvement mode, may involve small adaptations of the model code to manage data or scenarios differently from those currently proposed; these adaptations must then be made within the development environment of the Ocelet platform for more flexibility. This last mode is used for a posteriori evaluation of simulations made for a growing season, once crop statistics are available in the various countries, or to analyze/evaluate the impacts of climate change. The objective is to continuously improve the SARRA-O model over the years, taking into account past growing seasons and advances in the various fields to which the model appeals: remote sensing, meteorology and climatology, agronomy.

A. Diagnostic Mode

AGRHYMET publishes a monthly bulletin for monitoring the agropastoral campaign in West Africa (WA) (maps extracted from the AGRHYMET bulletin, 2017). A section of the bulletin is dedicated to describing the crop situation since the beginning of the campaign and any recommendations from experts. Like most crop models, a large number of output variables are used to describe the state and functioning of the soil (e.g., soil water content, evaporation) and vegetation (e.g., leaf index, stem and leaf biomass, transpiration, water stress indicator) (cf. Fig. 1).

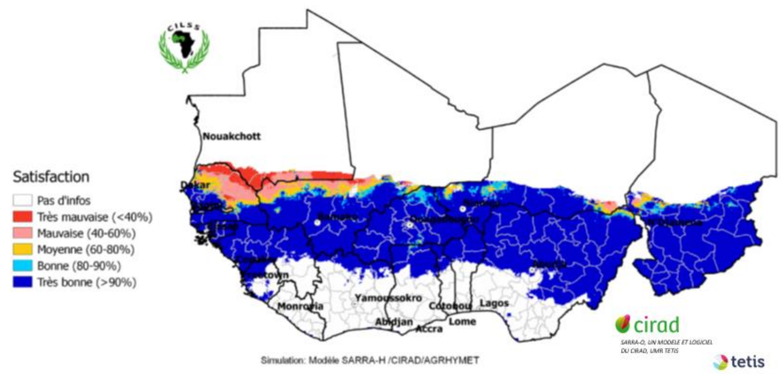

Fig. 1: Water stress indicator, plant water satisfaction

Among the information provided by the SARRA-O model is the simulated sowing date (cf. Fig. 2) based on the current year and the crop status during its juvenile period: depending on the start of the season, there may be plant mortality and thus one or more re-sowings. The sowing date is also called a successful sowing date to distinguish it from sowing dates that may have failed. This ability of the model to search for sowing dates based on soil moisture conditions and absence of drought periods immediately after is very important in these regions. Indeed, from one year to another, in the same location, the onset of the rainy season can vary by several months. And as observed here, during the same year, the onset of the rainy season varies, depending on latitude, from January/March to mid to late July.

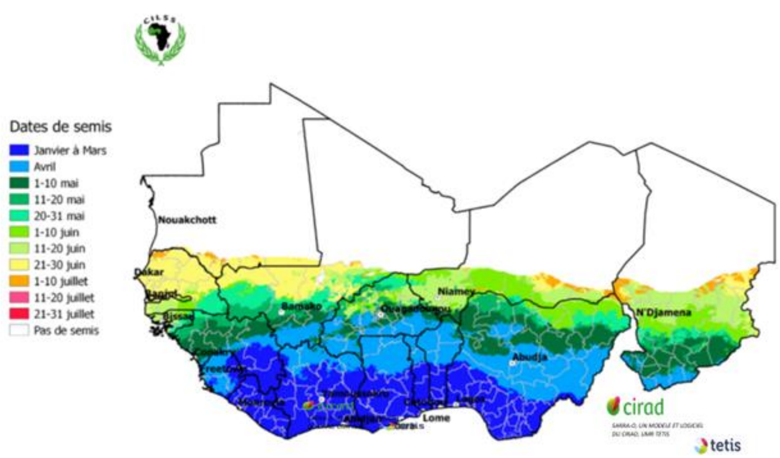

Fig. 2: Successful sowing date for the 2017 season

For each selected variable, the values at each pixel are saved in a raster file depending on the chosen time step for the outputs. These maps, in GeoTIFF format, can easily be finalized to facilitate the interpretation of information for decision-making. We recommend the use of the QGIS mapping software, which is free and open-source, for which several predefined formats and presentation modes adapted to the output variables (legends... logos...) are proposed during training sessions. The maps presented to you have been finalized using QGIS.

B. Forecast Mode

At the beginning of the season, AGRHYMET bulletins focus on crop establishment (successful sowing dates), crop water satisfaction levels, available soil water stocks, etc. These indices are monitored throughout the cropping season. By mid-season, it is possible to propose a series of yield prediction indices (Refer to the West Africa Agropastoral Campaign Monitoring Bulletin; August 2018: http://agrhymet.cilss.int/index.php/bulletins/).

The selected indicators are yield anomalies rather than estimates of absolute potential yields. The yield anomaly has the advantage of being able to be compared relative to previous situations, from 0 to 100%, and is easier to interpret than an absolute yield.

Equation : $AnomalieRdti = \frac{d\left(Rdti - Moy(Rdt)\right)}{Moy(Rdt)}$

Equation: Yield Anomaly = (Yield - Mean(Yield)) / Mean(Yield)

Moy(Rdt) = average of simulated yields over the chosen previous years' series.

Rdt_i = simulated yield for the current year (current year)

The period over which the average is calculated depends on the desired analysis. The examples below present several periods depending on the analysis conducted.

- Estimation of yield at flowering: You need to choose the "RdtPot" output variable, which should be understood as the yield at flowering, i.e., the yield that can be obtained at harvest under the condition of no stress until that date. This variable is the yield calculated at the flowering date, which is reached around the midpoint of the cropping season. To calculate the yield anomaly at flowering, you need to have chosen the same "RdtPot" output over a previous period of thirty years. You thus have at your disposal 30 images of flowering yields from TAMSAT data where each pixel (cell) has a resolution of 3.7 km * 3.7 km. You need to calculate the average of the flowering yields for the 30 previous years (Mean(Yield) in the equation) to be able to perform the calculation of the yield anomalies at flowering that you have obtained for the current year.

- Probabilistic forecast of harvest yields during the cropping season: You should choose the "Rdt" variable as the output, which is the simulated yield at harvest date. This date actually corresponds to the date of physiological maturity allowing this harvest, with the actual harvest potentially occurring later. To simulate this yield, from the chosen date during crop development, the calculation is extended until the harvest date using rainfall from previous years. It is recommended again to choose a period of the same duration, with 30 years being the norm in meteorology. Similarly, you obtain 30 raster images of probable yields at harvest (see details below). In this series of yields, you look for a determined occurrence, the yield value for which one can expect to obtain a yield equal to or greater than this value. Usually, quartiles of 75% or 25% are proposed; here, we recommend choosing occurrences at 80%, 50%, and 20%, which can be translated as the probability of obtaining at least this yield in 8, 5, or two years out of 10, which is much more explicit for the general public. Again, it is advisable to apply the anomaly calculation method based on the selected occurrence probabilities.

- Estimation of yield at harvest date: You also need to choose the "Rdt" variable. In the example, the anomaly calculation for the current year was performed over the past 5 years, for which yields were simulated (output variable "Rdt"). The above equation is then applied.

To carry out these treatments, scripts developed under the R programming environment are available and distributed during training sessions, as well as various files related to QGIS.

SARRA-O allows for the generation of four different yield indicators used for predictive purposes. The first three do not rely on meteorological or climatic forecasts. The last indicator uses these climatic predictions:

- Estimation of yield at flowering: This yield estimation, to distinguish it from others, is termed as the flowering yield (output variable "RdtPot") and is obtained approximately 1 to 2 months before the harvest date. Each cultivar has a potential yield under optimal conditions, without harmful insects or diseases, and without water constraints. However, water constraints can impact yield during the reproductive phase, the phase of reproductive organ development and flowering, which determines the number of grains. Thus, if the plant has experienced stress, it will produce fewer flowers, fewer grains, and its maximum attainable yield will have decreased by this date. This allows for the identification, at the flowering stage, of areas that have already been particularly affected and to estimate from this period the affected areas and the impact on the maximum attainable yields at the end of the season. From this date, the simulated yield can only be equivalent or lower if stresses occur. The map of potential yield anomalies at flowering (Fig. 3, top map) shows the areas that have already been impacted by periods of stress (orange). It is observed that these have extended to the harvest date (Fig. 3, bottom map). These maps are very useful for assessing the attainable yields during the season and highlighting areas in unfavorable situations, thus requiring special attention.

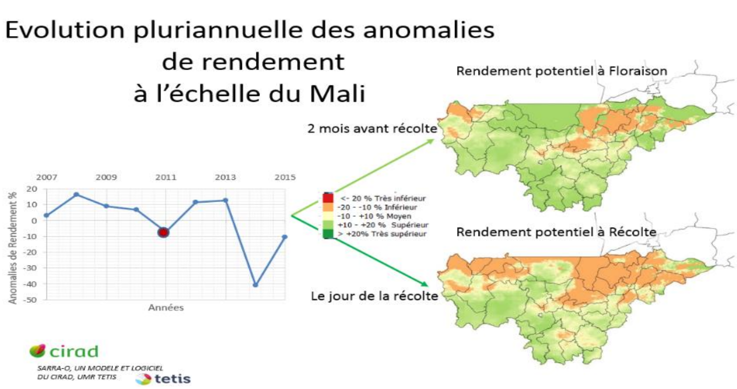

Fig. 3: Anomalies of yields at flowering date and at harvest date (physiological maturity)

Probabilistic forecast of harvest yields during the cropping season: This index relies on probabilistic analysis methods and allows for the estimation of potential yields (variable "Rdt") based on their probability of occurrence. Simulations are carried out at each pixel (cell) for the current year. Since the end of the season is unknown, climatic data from previous years up to the harvest date are used. It is recommended to choose a thirty-year period, resulting in 30 images of probable yields corresponding to the end of the cropping season of previous years that reflect the climate variability in each location (pixel).

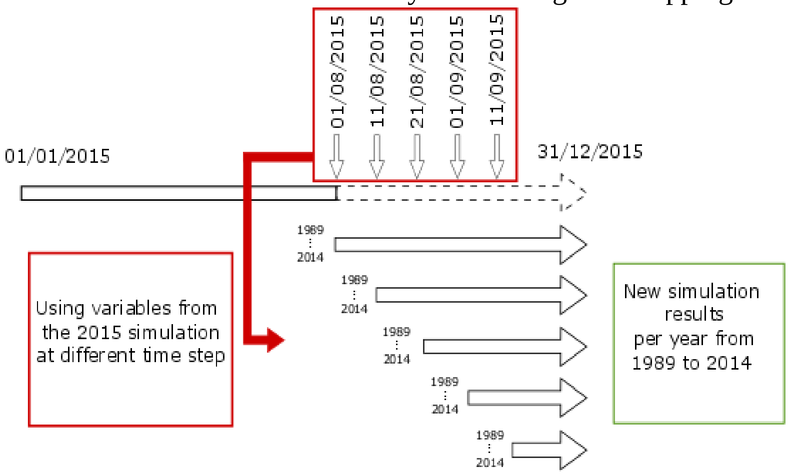

The simulation process for a pixel proceeds as follows:

The figure below (Castets et al., expected 2019) illustrates the simulation steps for the year 2015, considered here as the current year. In this example, we have data for the current year up to 08/01/2015, allowing for the simulation of the climate's impact on the crop since its sowing date. To complete the current year, which is still unknown, we finalize the simulation by retrieving, for each simulated pixel, data from 1989, which then gives us a yield. The same process is then repeated for each year from 1990 to 2014.

In the case of TAMSAT, we have a series starting in 1989 that, for each simulated pixel and for each year, performs simulations up to the harvest date (physiological maturity) and simulates a harvest yield. Thus, for each simulated pixel, for the period from 1989 to 2018, we can simulate 30 probable yields that take into account the observed climatic variability at that location : for all simulated pixels (600,000 in the case of West Africa), we have 30 simulated yields for each pixel, resulting in 30 images of yields. We then calculate, for this series of probable yields, occurrences at 80%, 50%, or 20%, for each pixel, corresponding to a probability of occurrence of 8, 5, or 2 years out of 10.

For the next ten-day period, on 08/11/2015, as soon as we obtain the information, we reproduce all the treatments. As we approach the harvest date, the difference in yields between each end of the year reduces until it disappears.

- Estimation of yield at harvest date : At the simulated physiological maturity date, a yield map is available from which it is possible to calculate the simulated yield anomaly for the current year. In Fig. 4, this anomaly was calculated from the average of the previous five years (for example, 2016 compared to 2011-2015). Five years correspond to the period during which it is estimated that individuals have a more reliable memory of the series of events that occurred in the past, and therefore for farmers, their yields obtained in the last 5 years.

This map (Fig. 4), obtained at the end of the cropping season, provides overall information covering multiple countries. Several large areas appear in greater deficit than others (orange), especially in the western zone as well as in Côte d'Ivoire and Niger.

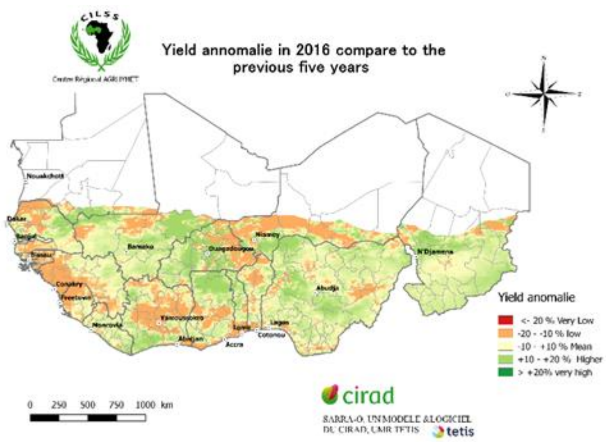

Fig. 4: Anomalies of simulated yields based on the previous 5 years

- Forecasting harvest yields with seasonal meteorological forecasts : We utilize outputs from meteorological forecast models, these forecasts, at daily time steps, are used to complete the simulation up to the simulated harvest date (physiological maturity), allowing for the generation of a yield forecast map (variable "Rdt"). Similar to the previous methods, we can then provide a map of anomalies based on the selected past period. The usefulness of using these seasonal forecasts has already been demonstrated using the SARRA-H version of this model (Roudier P. et al. 2016).

C. Analysis and Improvement Mode

This mode is exploited outside the cropping season without the semi-real-time constraints of the SAP. As with any crop model, it is necessary to ensure verification and continuous improvement of the system's performance level. With the graphical interface, it is possible to analyze the effect of different farming strategies and trends over long historical series, taking into account their geographical location : soils and climatic constraints. It is therefore possible to analyze the effect of intensification/fertility levels, sowing strategies (early... late), choice of cultivars, etc. This allows for the creation of agro-climatic zoning and improvement of simulation scenarios through new thematic maps in the long term. Thus, the farming strategies (dates, cultivars...) represented through simulation scenarios are better adapted to the environmental constraints of these areas : for example, instead of proposing the same cycle length everywhere, only cultivars with a shorter cycle length adapted to this constraint will be simulated in areas where the growing season is too short.

Furthermore, sensitivity analyses and tests need to be regularly conducted regarding:

- Sources of new input data, especially in the context of remote sensing (new sensors, etc.),
- Improvement of climate data estimates and/or climate forecasts and climate change (bias correction, etc.),
- Traditional model evolutions. Evolution translates into new cultivars, modifications of parameter values (based on new experimental and/or farmer survey data), modifications in the formulation of certain model processes, etc.

This last research and development (R&D) activity is conducted by Cirad in collaboration with AGRHYMET and other research organizations. These studies can be conducted as simple collaborations or as part of international projects that may address broader themes. This latter aspect will not be developed here; only the currently available capabilities provided by the interface will be detailed. And a series of analysis modes and results will be presented at the end of this manual.

II. Diagnostics

This diagnostic mode involves the ability to continuously monitor crop development throughout the growing season and thus obtain essential climatic data in semi-real-time, within a few days. In our case, TAMSAT and ECMWF data are accessible with a delay of less than 10 days, allowing for continuous monitoring and dissemination with a short, known, and constant delay.

The diagnostic mode allows for highlighting various aspects throughout the crop development:

- Crop establishment (sowing dates), as well as information concerning the number of failed sowings which may indicate significant issues (seed availability...).
- Drought pockets, their areas, and estimating their impact on crop development.
- Showing the geographical disparity of sowings, which can be early or late compared to previous years.
- Available water stocks for crops, allowing for estimating risks for the upcoming 10 days or planning actions (e.g., supplemental irrigation).
- The crop's condition since sowing through indicators of stress, growth estimation (Cstr, LAI, biomass...).

In each monitored area (region, country, administrative division), this monitoring mode allows for continuous estimation and evaluation, in semi-real-time and geo-localized, of the impacts on crops that may affect yield development.

A. Sowing Date

The simulated sowing date is the day when the water available in the surface reservoir (here 20 cm) is greater than or equal to 10 mm. Sowing is considered successful if the crop is not subjected to significant water stress during its juvenile period (20 days), resulting in a decline in biomass for several days.

A strategic piece of information for monitoring a cropping season is the map of successful sowings, showing whether the season has started early, late, or normally in different locations of the studied area. The map of simulated sowing dates using the model is closely linked to the onset of the current year's monsoon, allowing or not allowing sowing, and then to the water constraints (dry period) experienced by the crop, which can lead to mortality in its juvenile phase and involve re-sowing. It can be considered as the reference date from which farmers define their sowing strategy for this cropping season (p. 12, Fig 2).

Sowing Strategies:

The model allows for the consideration of farmers' sowing strategies, including the notion of early or late sowings, by defining a delay in days. The search for the sowing date is conditioned by the average sowing date at each point, and the delay is defined in days.

The average sowing date is defined at each point by the thematic map of the average start of the cropping season. This map was obtained through analysis of ground station network climatic series conducted by AGRHYMET. In the case of searching for the earliest sowing date, the deviation from the average sowing date must be significant. In the case of West Africa, it is recommended to start the simulation by defining a delay of more than three months (-90 days), "sowing date," to initiate the search for the sowing date. If one wishes to take into account staggered sowing strategies, multiple simulations can be performed at each point (pixel). Indeed, with a resolution of 3.7 km per pixel (TAMSAT), this covers several cultivated plots and/or farms in these regions. Depending on the climatic zones, sowings can be spread over more than a month (southern latitude). One can define a delay of plus or minus 20 days and thus evaluate the impact of different sowing strategies (see p. 12).

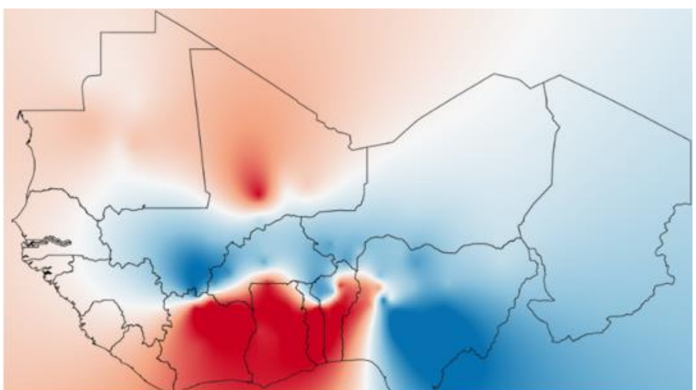

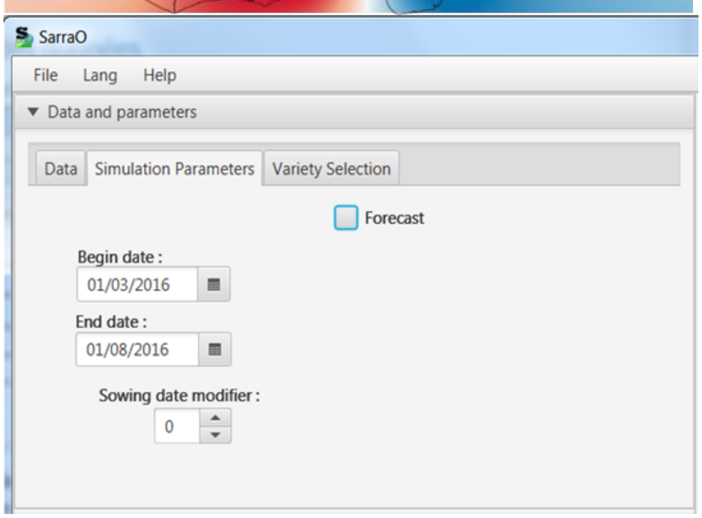

B. Crop Water Stress Index

Throughout the cropping season, the water status of crops is carefully examined, as prolonged water stress can have significant impacts. For cereals, two critical phases have been defined that have a marked effect on yield: 1) the reproductive phase, from panicle initiation to flowering, the phase of reproductive organ development defining the number of flowers and thus the number of grains, 2) the grain filling phase. The index used in the model to express crop water stress is the Crop Water Stress Ratio (CSTR), calculated as the ratio of actual plant transpiration (mm), constrained by available soil water, to potential transpiration corresponding to its needs (mm). This value, calculated daily, ranges from 0 to 1. CSTR index maps can be produced at any time during the season (p. 12, Fig 1). These maps can be obtained either every 10 days (10-daily) or since sowing (Annual). They represent the average stress experienced over the chosen period.

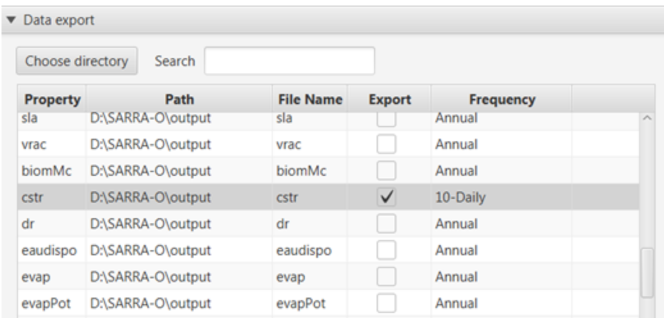

III. Yield Forecasting

- Forecast at flowering :

The model provides an initial forecast at the flowering date, which is defined here by the variable RdtPot, to be interpreted as the potential yield at the flowering date. Indeed, this forecast integrates water stresses experienced since sowing and their impact : 1) on the vegetative development of the crop, 2) during the sensitive phase of development, the reproductive phase (RPR), during which the number of reproductive cells develops. In the case of cereals, this results in flowers that determine the number of grains. In case of stress, the number of reproductive cells will be reduced, directly impacting the maximum yield to come, regardless of environmental conditions until harvest.

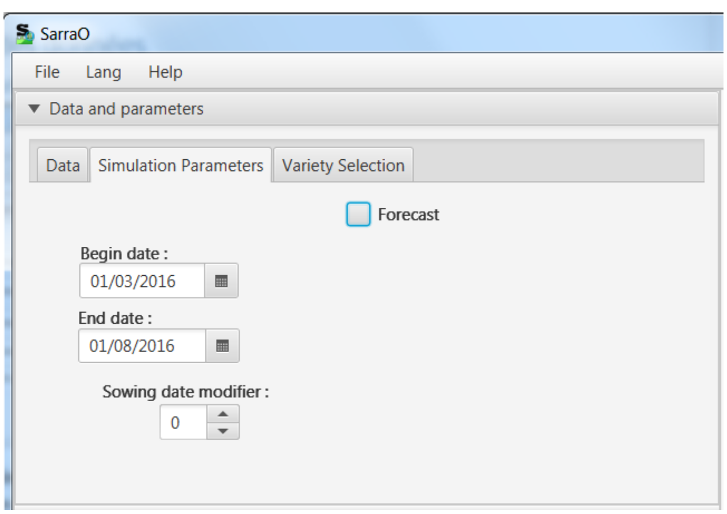

- Forecasts until harvest :

Several forecasting methods can be used: either by having climate forecasts adapted to the model's input format, or by using historical climate series giving a probability of future yields and taking into account climate variability at each point.

a) Climate forecasts:

It is sufficient, for now, to adapt the file naming and format to the established standards of TAMSAT and ECMWF, allowing for the compilation of end-of-season climate forecasts and defining the end date of simulations beyond the harvest date. Note: In the future, interface adaptations are planned to facilitate the use of forecast data with various naming conventions, with the formats currently being in GEOtiff format for spatial data.

b) Probabilistic yield forecasts (historical series):

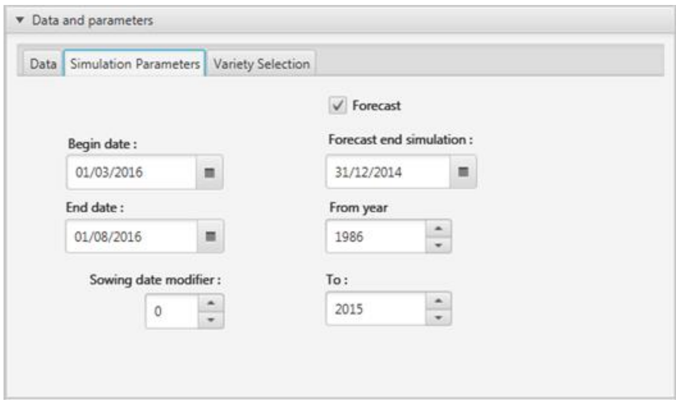

For this option, you need to complete the information that appears when you select the "Forecast" button.

In this example, we are approximately in the middle of the growing season, in the month of August, which corresponds more or less to the flowering stage for the Sudano-Sahelian zone (bordering the desert). After selecting the "Forecast" button, several new parameters appear. Regarding the end date of simulations for the forecast mode, it is recommended to set a date beyond the traditional harvest date (note: do not consider the year, only the day and month are retained), and then define the historical period that will allow for the compilation of the end of the current year with the climatic data from each year of this historical series. To conduct this probabilistic analysis, it is advisable to define a previous period of 30 years, identical to that chosen in climatological analyses. (Note: in the case of TAMSAT and ECMWF, the historical period goes back to 1989).

IV. Analyses and Improvements

In this final chapter, we will briefly present some results of model analysis and sensitivity studies, primarily intended to be didactic, to pose a set of questions, to propose outlines of analysis results and tests attempting to answer them, and above all, to open doors.

A. Seeding Strategies: Species & Varieties vs Environment

The model enables searches for seeding dates on all pixels based on seeding success criteria and a starting date. This starting date for the search is defined from the crop season start map (p. 18). Two seeding strategy scenarios have thus been defined: first, starting the search from this starting date (Fig. 5), then a second scenario where it is assumed that the farmer waits about 15 days from this date (Fig. 6), for example, to prepare the soil through plowing after the first rains to avoid tiring the oxen.

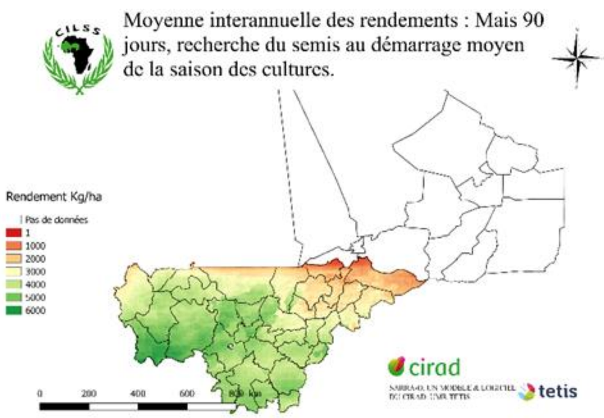

[Fig. 5: Seeding search from the average date]

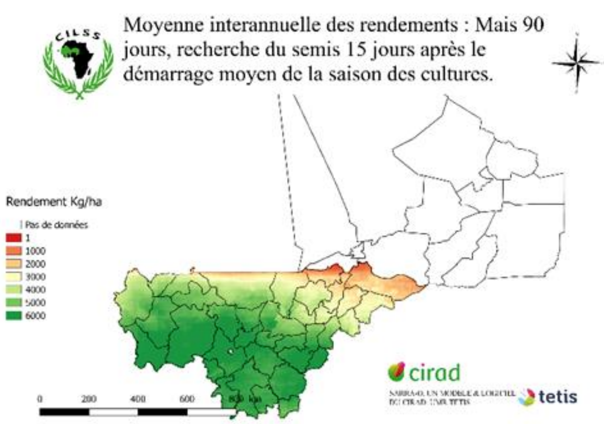

[Fig. 6: Seeding search 15 days later]

The simulated yields correspond to an optimal technical situation and fertility level (I4) as well as for a variety commonly used in these regions (non-hybrid). It should be noted that regardless of the seeding strategy, the Northern zone is not suitable for maize (red, orange). Opting for a later seeding strategy in the zone traditionally known for maize cultivation (green) results in a significant increase in yield and less spatial variability. These analysis results can therefore help better define the most suitable areas with fewer risks based on associated practices.

B. Capturing Yield Variability: Simulating Actual Yield?

Within the framework of the European FP7 SIGMA project (Stimulating Innovation for Global Monitoring of Agriculture and its Impact on the Environment; 2013-17), surveys and measurements were conducted in peasant communities in Burkina Faso, focusing on two cereals: maize and sorghum. This work was carried out over three years in six villages with monitoring and measurements in approximately 180 plots per year. To capture the variability of yields measured in peasant fields, ranging from 500 to 5000 kg/ha for maize, we defined four levels of intensification (technical and fertility levels from I1 to I4) to simulate yields and verify the predictive capacity of the model on observed yields:

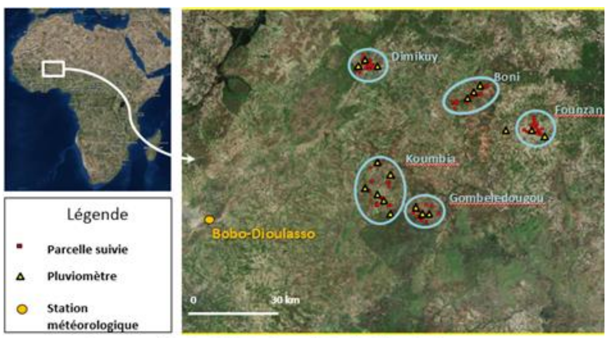

Carte : Localisation de la Province de Tuy (Burkina Faso)

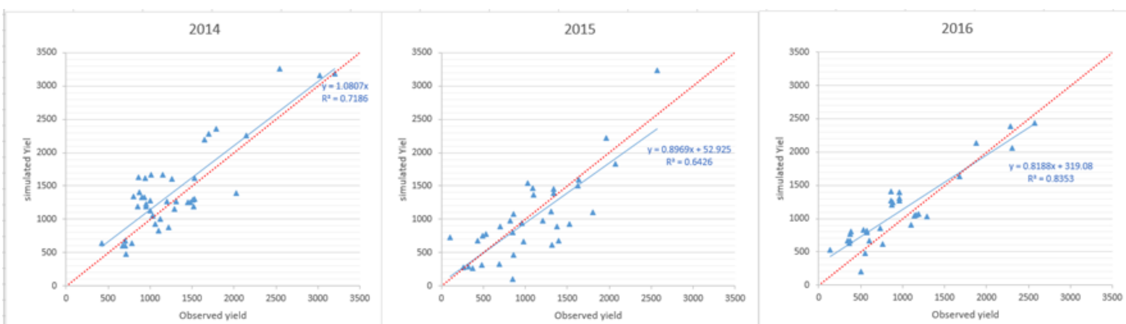

[Fig. 7: Correlation between simulated and observed maize yields measured in peasant fields (2014 to 2016)]

The correlations obtained are high or correct given the very large variability of yields, and especially hold true for other years: R^2 of 0.71 in 2014, 0.64 in 2015, and 0.83 in 2016. To reproduce actual yields through simulations in peasant communities, we conducted a series of four simulation sets across Burkina Faso. Fig. 8 shows the spatial variability of yields for the same simulated year based on the four levels of intensification (I1 to I4). The map titles indicate the minimum and maximum values of simulated yields for each level of intensification. Fig. 9 is obtained by applying a weighted sum of yields calculated for each pixel and for these four levels of intensification. The polygon on the map delimits the area of the six villages. By averaging the simulated yields for pixels within the polygon, the simulated yield is close to the observed (2.8 Sim. and 2.3 Obs.).

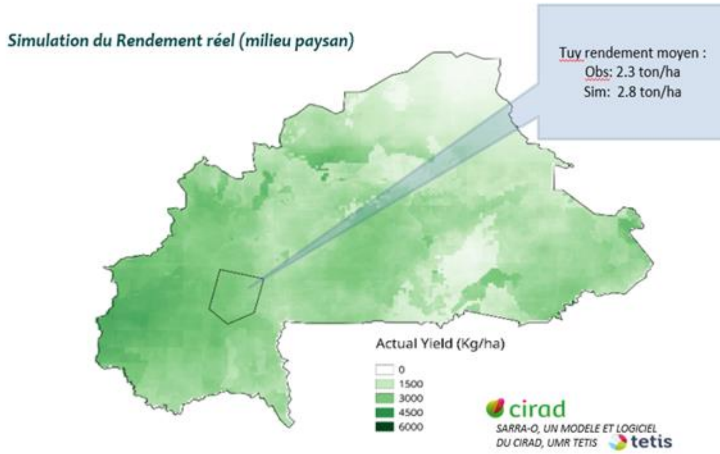

Fig. 8: Maps of simulated yields based on intensity levels

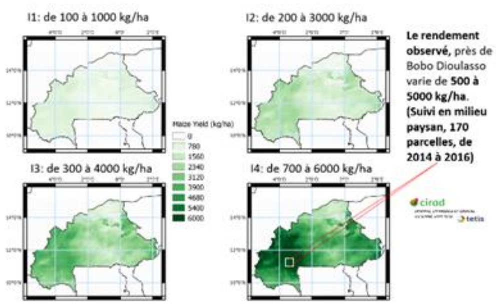

Fig. 9: Map of simulated actual yields

C. Yield Gap Analysis: The Yield Gap!

As part of the SIGMA project, one of the study themes was to estimate the gap between actual yields and potential yields obtained under controlled conditions and in optimum situations. This analysis is traditionally done by comparing observed yields with simulated yields in optimum situations, but without irrigation input (water-limited), as shown in this diagram. The terminologies have changed since 2013; those currently used to distinguish situations are:

i. Absolute for crops not limited by water,
ii. Potential for water-limited crops, and
iii. Actual for on-farm yields.

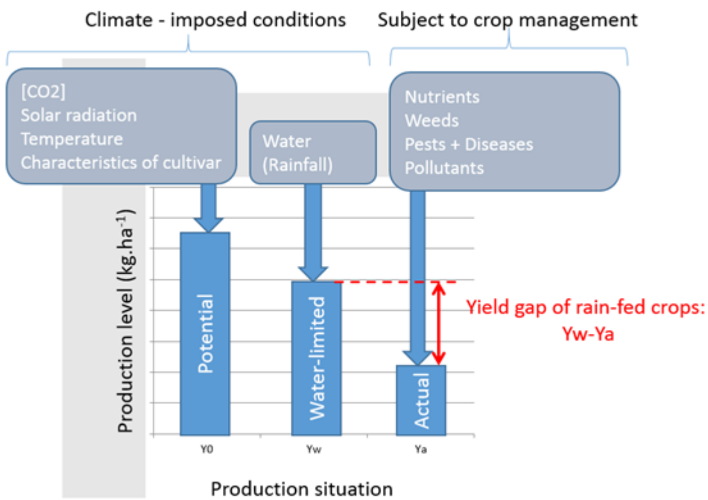

[van Ittersum & al., 2013. Yield gap analysis with local to global relevance.]

The interest of the method proposed here is that it utilizes the predictive capacity of the model to simulate yields in peasant communities. This approach provides a much finer and more homogeneous spatial distribution over the studied territories, while also integrating the effect of soil. Areas showing highly fragmented yield anomalies highlight the effect of soil characteristics: water storage capacity, maximum rooting depth, and runoff potential (Fig. 10).

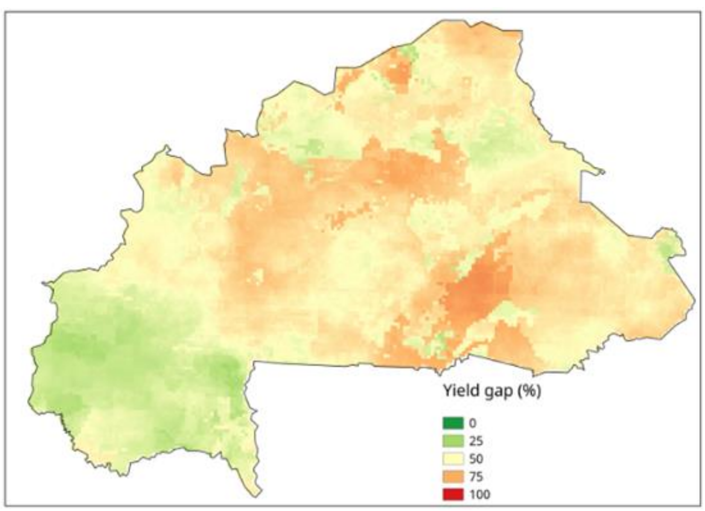

[Fig. 10: Map of gaps between potential and simulated actual yields]

As specified in the diagram above, an analysis can also be conducted without considering water constraints. This second analysis aims to show areas where it will not be possible to achieve the cultivar's potential yield without additional irrigation input: absolute yield (Fig. 11). The Northern zone is the one that highlights the most water constraints. Note the effect of soil in these constraints, which is also evident in the Southeast zone. It is possible, of course, to obtain the map of additional irrigations required to achieve this absolute yield.

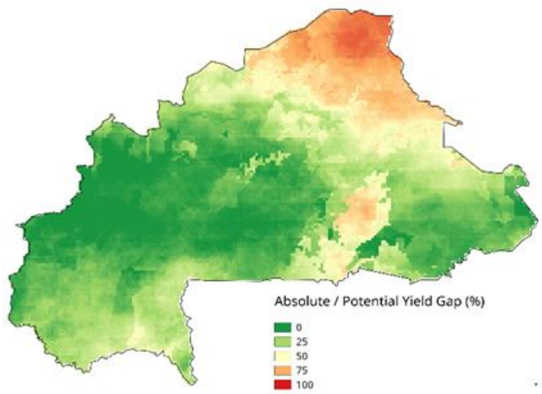

[Fig. 11: Map of gaps between absolute and potential yields]

D. From Yield to Production

One of the objectives of the LAUREL project (Land Use Planning For Enhanced Resilience of Landscape, 2017-2019), financed by the World Bank, concerns the estimation of production for various crops. Production (Fig. 12, Crop production) is obtained by combining cultivated areas, estimated by remote sensing (Fig. 12, Crop surface), with maps of simulated yields obtained based on crops and practices (Fig. 12, Crop yield (I2): simulated yields for a 90-day maize with low intensity). Starting from this state in 2015, simulations taking into account climate change and forecasts of changes in cultivated areas have allowed for the estimation of production trends by 2050.

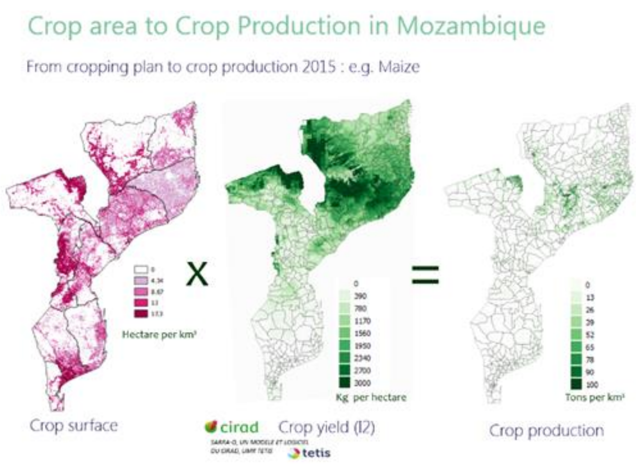

[Fig. 12: Maize production map (I2)]

E. Thematic Maps and Simulation Scenarios

Figures 5 and 6 (p. 21) showed the effects of different seeding strategies (scenarios) on yield estimation. Crop calendar management must adapt to climatic constraints such as the start of the season, its duration, and the periods most suitable for crop management constraints. The example presented here (Fig. 13, right) demonstrates the possibilities offered by the use of historical daily rainfall series estimated from satellites. It is possible, through the model's estimation processes of successful seeding dates, to obtain maps of seeding onset early in the crop season. Many of the methods used to estimate growing seasons only consider climate or precipitation. The method proposed here combines the effect of climate, estimated from time series of satellite images (precipitation, evapotranspiration, temperature, global radiation), and soil on plants. Thus: i) it no longer depends on the quality of the ground station network, which is unevenly covered, has low coverage, and poor historical series quality (Fig. 13, left), ii) it also takes into account soil characteristics, iii) and finally, it is based on plant biological processes and the impacts of meeting its water needs, both for emergence and the juvenile phase, which may induce reseeding.

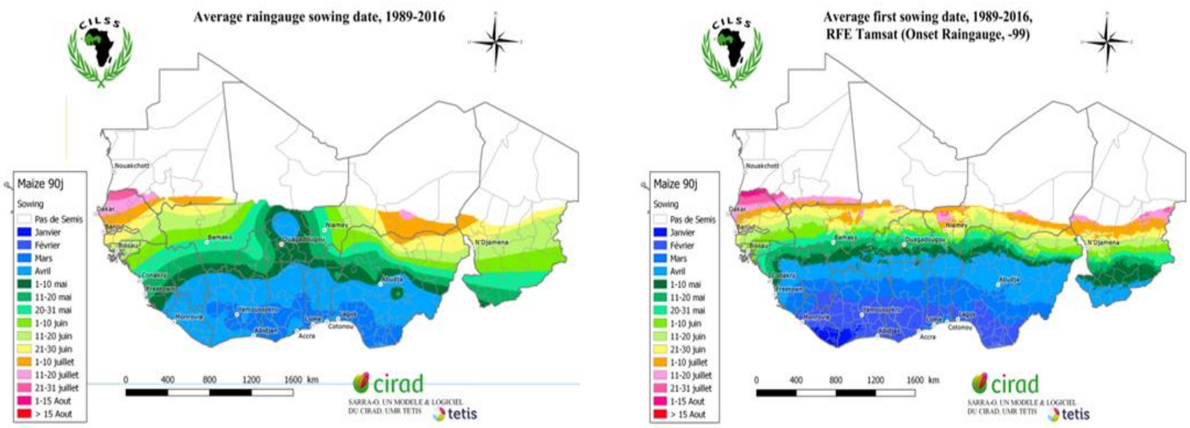

Fig. 13: Map of earliest interannual average seeding dates: 1) on the left, estimation of seeding dates using ground station network (Sivakumar method), 2) on the right, simulation of earliest seeding date by the model with rainfall data estimated by Tamsat.

This example highlights both the problems of accessibility and availability of data as well as the importance of a well-covered ground station network, which has declined in recent decades. The effects of poor distribution of stations are clearly visible through the bubble effects on the left map. The new map, due to the continuous meshing of satellite image pixels, does not present the same problem. Rainfall isohyets are more regular, with areas reflecting the soil effect, such as above Bamako, for example. While this distribution is more consistent with our understanding of the dynamics of rainfall phenomena movement, such as the movement of the Inter-Tropical Convergence Zone (ITCZ), the quality of rainfall estimations from satellites, which are calibrated by the available ground station network, must also be questioned and verified [Pellarin T. et al., 2019; Ramarohetra et al., 2013; Maidment et al., 2017].

F. And much more...

In the context of research and development work conducted through projects and/or partnerships with various institutes and universities, several lines of study are ongoing or have already produced various results, including academic outcomes: over 50 publications in peer-reviewed journals.

Initially, issues of scaling and their impact on simulations were addressed (Baron et al., 2005; Sultan B. et al., 2005; Oettli P. et al., 2011). Farming practices and adaptations have also been studied (Traore S. B. et al., 2011; Marteau R. et al., 2011; Philippon N. et al., 2016), as well as the importance of seasonal forecasts in early warning systems (Roudier P. et al., 2011; Roudier P. et al., 2016).

The impact of climate change has also been extensively studied, leading to a large number of simulations with the SARRA-H&O crop models across several countries in West Africa, comparing various climate change models (Guan, K. et al., 2015; Sultan B. et al., 2013; Parkes B. et al., 2018). As part of the international AgMip project, since 2011, Cirad has participated in a series of studies comparing the SARRA-H model with approximately 29 other models for maize and addressing various issues such as the impact of CO2 concentration conducted in the field (Durand J-L et al., 2017), and the predictive capacity of estimating evapotranspiration (Bruce A., 2019). The latest ongoing study concerns the African continent and the models' ability to simulate yields in situations with low fertilization levels, with each advancement being integrated into the spatialized version of SARRA-O.

The spatialized version of the model opens the doors to a better utilization of various sources of satellite data. These data, although regularly distributed, reliable, and repetitive, are not without bias (Ramarohetra et al., 2013). Supported by the University of Grenoble, the use of SMOS data (surface soil moisture) has already shown promising results (Gibon F. et al., 2018, and thesis). Its use in near-real-time is currently being implemented and should improve the performance of rainfall estimation models based on satellite imagery (Pellarin T., 2019). Other satellite sources have been analyzed and compared to the model in an assimilation and/or verification approach (Vintrou E. et al., 2014, Leroux et al., 2016, Jahel C. et al., 2018, Leroux et al., 2019).

The use of new satellites (Sentinels...), offering better resolution, opens up promising prospects for better assimilation of these data during the growing season, allowing for improvement and/or comparison of different methods: i.e., start of the vegetation growth season, harvest periods...

Acknowledgments

The SARRA-O software is the result of a long journey and a great deal of experience. The history regarding these developments shows the diversity of actions around the SARRA-H model and software and also allows us to thank all those who participated (https://sarra-h.teledetection.fr/Historique.html). For this new version, integrating satellite images and data from climate change models, it is important to highlight a group of colleagues, some of whom have been there from the beginning and others who have been invaluable supporters. First and foremost, we must thank the farmers and peasant organizations who welcomed us and contributed significantly to various projects, notably AMMA and Sigma (European projects). There has also been strong support from interns, postdocs, and doctoral students who have helped us advance and better understand and translate the diversity of what we are trying to capture. For postdocs and doctoral students, it has been a pleasure to mention them throughout this brief manual in relation to the results of their work. For interns, we would like to thank in particular: Stella Guillemot, Koladé Akakpo, Cyrille Ahmed Midingoyi, and Thomas Gendron.

There are numerous scientific partners, and we wish to acknowledge their institutions through them. Particularly AGRHYMET, which welcomed and supported us, we extend special thanks to Seydou B. Traore, Agali Alhassane, and Henri Songoti for their strong and consistent participation and commitment. The national meteorological partners from various ECOWAS countries with whom we were able to dialogue, verify, and test the software in the context of training (notably the Crews project in connection with WMO), as well as partners from EMBRAPA in Brazil (GEOABC-Capes Cofecub project).

In the context of studies on climate impacts and climate change, we must mention Albert Olioso (Inra), Thierry Pellarin (CNRS, IRD, Univ. Grenoble), and Benjamin Sultan (IRD).

CIRAD and UMR TETIS have allowed us to have this long time to work on all these developments, notably with CIRAD colleagues: Agnès Bégué, Danny Lo Seen, and Camille Jahel, who during her thesis paved the way and participated in the implementation of this new version, along with Louise Leroux (CIRAD, UPR Aida).

VI. Some Bibliographical References

Baron, C., Sultan, B., Balme, M., Sarr, B., Traore, S., Lebel, T., Janicot, S., Dingkuhn, M., 2005. From GCM grid cell to agricultural plot: scale issues affecting modelling of climate impact. Philosophical Transactions of the Royal Society B: Biological Sciences, 360(1463), 2095–2108. http://doi.org/10.1098/rstb.2005.1741

Bruce A. Kimball, Kenneth J. Boote, Jerry L. Hatfield, Laj R. Ahuja, Claudio Stockle,Sotirios Archontoulis, Christian Baron, Bruno Basso, Patrick Bertuzzi et al., 2019. Simulation of maize evapotranspiration: An inter-comparison among 29 maize models, Agricultural and Forest Meteorology, https://doi.org/10.1016/j.agrformet.2019.02.037

Castets M., Baron C., Traore S.B., Jahel C., Songoti H., Degenne P., Alhassane A., Lo Seen D, 2016. Assessing agricultural practices in highly variable environments: SARRA-H spatialized crop model for West Africa. AgMIP6 Global Workshop, Montpellier, France.

Degenne, P, Lo Seen, D, Parigot, D, Forax, R, Tran, A, Ait Lahcen, A, Curé, O, Jeansoulin, R, 2009. Design of a domain specific language for modelling processes in landscapes. Ecol. Model. 220(24), 3527–3535.

Degenne P., Lo Seen D., 2016. Ocelet: Simulating processes of landscape changes using interaction graphs. SoftwareX, 5:89-95.

Dingkuhn M, Baron C, Bonnal V, Maraux F, Sarr B, Sultan B, Clopes A, Forest F, 2003. Decision support tools for rainfed crops in the Sahel at the plot and regional scales. T.E. Struif Bontkes, M.C.S. Wopereis (Eds.), Decision support tools for smallholder agriculture in sub-Saharan Africa: a practical guide, IFDC, Muscle Shoals, USA, pp. 127-139

Durand J.L.,Kenel Delusca ,Ken Boote, Jon Lizaso, Remy Manderscheid, Hans Johachim Weigel, Alex C Ruane, Cynthia Rosenzweig, Jim Jones, Laj Ahuja, Saseendran Anapalli, Bruno Basso, Christian Baron, Patrick Bertuzzi, Christian Biernath, Delphine Deryng et al., 2017. How accurately do maize crop models simulate the interactions of atmospheric CO2 concentration levels with limited water supply on water use and yield? European Journal of Agronomy, http://dx.doi.org/10.1016/j.eja.2017.01.002

FAO (2016), Crop Yield Forecasting: Methodological and Institutional Aspects"

Gibon F., Thierry Pellarin, Carlos Román-Cascón, Agali Alhassane, Seydou Traoré, Yann Kerr, Danny Lo Seen, Christian Baron, 2018. Millet yield estimates in the Sahel using satellite derived soil moisture time series, Agricultural and Forest Meteorology, https://doi.org/10.1016/j.agrformet.2018.07.001

Guan, K., B. Sultan, M. Biasutti, C. Baron, and D. B. Lobell, 2015. What aspects of future rainfall changes matter for crop yields in West Africa?, Geophys. Res. Lett., 42, 8001–8010, https://doi.org/10.1002/2015GL063877.

Jahel C., Baron C., Vall E., Karambiri M., Castets M., Coulibaly K., Bégué A., Lo Seen D., 2017. Spatial modelling of agro-ecosystem dynamics across scales: A case in the cotton region of West-Burkina Faso, Agricultural Systems, http://dx.doi.org/10.1016/j.agsy.2016.05.016

Kouressy M., Dingkuhn M., Vaksmann M., Heinemann A., 2008. Adaptation to diverse semi-arid environments of sorghum genotypes having different plant type and sensitivity to photoperiod. Agricultural and Forest Meteorology, 148 (3) : 357-371.
http://dx.doi.org/10.1016/j.agrformet.2007.09.009

Louise Leroux, Mathieu Castets, Christian Baron, Maria-Jose Escorihuela, Agnes Begue, Danny Lo Seen, 2019. Maize yield estimation in West Africa from crop process-induced combinations of multi-domain remote sensing indices, European Journal of Agronomy https://doi.org/10.1016/j.eja.2019.04.007

Leroux, L., Baron, C., Zoungrana, B., Traoré, S. B., Lo Seen, D., & Bégué, A., 2016. Crop Monitoring Using Vegetation And Thermal Indices For Yield Estimates: Case Study Of A Rainfed Cereal In Semi-Arid West Africa. IEEE Journal of Selected Topics in Applied Earth Observations and Remote Sensing, 9(1), 347–362. http://doi.org/10.1109/JSTARS.2015.2501343

Maidment, Ross, Black, Emily, Tarnavsky, Elena, 2016. TAMSAT Daily Rainfall Estimates. University of Reading. Dataset. http://dx.doi.org/10.17864/1947.40

Maidment RI, Grimes D, Black E, Tarnavsky E, Young M, Greatrex H, Allan RP, Stein T, Nkonde E, Senkunda S, Alcántara EMU, 2017. A new, long-term daily satellite-based rainfall dataset for operational monitoring in Africa. Scientific Data, 4, 170063. http://dx.doi.org/10.1038/sdata.2017.63

Parkes B., Dimitri Defrance, Benjamin Sultan, Philippe Ciais, and Xuhui Wang, 2018. Projected changes in crop yield mean and variability over West Africa in a world 1.5K warmer than the pre-industrial era. Earth Syst. Dynam., 9, 119–134, 2018. https://doi.org/10.5194/esd-9-119-2018

Pellarin T., Roman-Gascon C., Baron C., Brocca L., Camberlin P., Prieto D.F., Kerr Y.H., Massari C., Panthou G., Perrimond B., Philippon N., and Quantin G., 2019 en cours. From SMOS surface soil moisture retrievals to near real-time rainfall estimates in Africa: the PrISM methodology.

Ramarohetra J, Sultan B, Baron C, Gaiser T and Gosset M, 2013. How satellite rainfall estimate errors may impact rainfed cereal yield simulation in West Africa. Agric. For. Meteorol., 180:118–31

Roudier P., A. Alhassane, C. Baron, S. Louvet, B. Sultan, 2016. Assessing the benefits of weather and seasonal forecasts to millet growers in Niger, Agricultural and Forest Meteorology, Volume 223, 15 June 2016, Pages 168-180, ISSN 0168-1923, http://dx.doi.org/10.1016/j.agrformet.2016.04.010

http://www.sciencedirect.com/science/article/pii/S0168192316302416

Sultan B, Roudier P, Quirion P, Alhassane A, Muller B, Dingkuhn M, Ciais P, Guimberteau M, Traore S, Baron C, 2013. Assessing climate change impacts on sorghum and millet yields in the Sudanian and Sahelian savannas of West Africa. Environmental Research Letters, 8:014040, 9 pages, http://dx.doi.org/10.1088/1748-9326/8/1/014040

Traoré, S. B., Alhassane, A., Muller, B., Kouressy, M., Somé, L., Sultan, B., Oettli, P., Siéné L., Ambroise C., Sangaré, S., Vaksmann, M., Diop, M., Dingkuhn, M., Baron, C., 2011. Characterizing and modeling the diversity of cropping situations under climatic constraints in West Africa. Atmos. Sci. Let. 7p., DOI: 10.1002/asl.332.

VII. Appendix: Description of Variables

A. Plant Parameters (Crops)

Parameters commonly used for calibration: all are measured or deduced from field monitoring (experiments or farmers)

Parameter	Functional Group	Unit	Default	Value Range	Description	Frequently Used
SDJBVP	Phenology and Photoperiodism	°C.d	400	200…1000	Phase 2: Duration in degree-days from emergence to panicle initiation (reproductive organs), vegetative development phase	Duration of the cycle in the absence of photoperiodism varies between species and varieties
SDJRPR	Phenology and Photoperiodism	°C.d	400	200…600	Phase 4: Duration in degree-days from panicle initiation to flowering (reproductive phase)	Same as above
SDJMatu1	Phenology and Photoperiodism	°C.d	400	200…600	Phase 5: Duration in degree-days from flowering to end of grain filling. Additional vegetative development for cereals.	Same as above
SDJMatu2	Phenology and Photoperiodism	°C.d	50	0…300	Phase 6: Duration in degree-days from end of grain filling to physiological maturity (harvest date). No more vegetative development, grain drying period.	Same as above
PPSens	Phenology and Photoperiodism	none	0.7	0.1…1	Photoperiod sensitivity. From 0.3 to 0.6 it is sensitive to PP, it disappears for values ranging from 0.7 to 1. See Dingkuhn et al. 2008; Euro.J.Agron. (Impatience model)	Definition of sensitivity to PP
SlaMin	Leaf Properties	kg/ha	0.0018	0.001…0.004	SLA (specific leaf area): Leaf surface/dry biomass. Final value (minimum) for the entire canopy.	Use with caution and only if you have measurements or based on literature
SlaMax	Leaf Properties	kg/ha	0.0060	0.004…0.008	Initial value (maximum) for the entire canopy.	Same as above
Kdf	Light Conversion and Extinction	none	0.5	0.3…1	Defines the extinction of diffuse solar radiation from the vegetation cover as a function of LAI. 0.4 =	Use with caution and only if you have measurements or based on literature.

Parameter	Functional Group	Unit	Default	Value Range	Description	Frequently Used
					straight leaves, 1 = horizontal leaves.	Variates little for cereals (0.4 to 0.6)
TxConversion	Light Conversion and Extinction	g/MJ	4 (C3), 6 (C4)	2…8	Radiation efficiency (RUE=epsilon-b) BEFORE maintenance respiration. This value can be up to 2 times higher than the RUE found in the literature, which is not based on assimilation but on biomass, and does not include root system and maintenance respiration. Important parameter!	Use with caution. Low variation within varieties of the same species. Fertilizer input and/or soil fertility strongly impact this conversion rate
KrdtPotA	Biomass Properties	kg/kg	0.4 … 1.1		Yield potential (equivalent to HI but in kg)	Between species and varieties
FeuilAeroPente	Biomass Properties	none	-9E-5… - 0.00018		Regression slope of leaf biomass distribution on aerial biomass	Between species and varieties

Rarely used parameters:

Default	Crop Parameters	Functional Group	Unit	Default	Value Range	Description	Used for
0.5	TxResGrain	Seed Properties	fraction	0.5	0.4…0.8	Fraction of grain weight mobilizable for	

Default	Crop Parameters	Functional Group	Unit	Default	Value Range	Description	Used for
						growth (emergence)	
	PoidsSecGrain	Seed Properties	g	0.028	0.01-0.05	Dry weight of a grain	Especially between species, use dry weight measurements of grains
50	SDJLevee	Seed Properties	°C.d	50	0…infinite	Phase 1: Duration in degree-days from sowing to emergence, when the soil is wet	Especially between species
10	TBase	Phenology and Photoperiodism	°C	10	0…15	Air base temperature allowing plant development	Rarely between species, rarely between varieties of the same species
25	TOpt1	Phenology and Photoperiodism	°C	25	15…30	Lower limit of the optimum thermal development plateau	Same as above
35	TOpt2	Phenology and Photoperiodism	°C	35	25…40	Upper limit of the optimum thermal development plateau	Same as above
40	TLim	Phenology and Photoperiodism	°C	40	30…50	Maximum plant development temperature (lethal temperature)	Same as above
0.17	PPExp	Phenology and Photoperiodism	none	0.2	0.1…1	Progressive attenuation of the response to photoperiodism rarely used. Default value 0.17	

Default	Crop Parameters	Functional Group	Unit	Default	Value Range	Description	Used for
13.5	SeuilPP	Phenology and Photoperiodism	h	13.5	14	Maximum day length limiting the PP response	
11.5	PPCrit	Phenology and Photoperiodism	h	11	10	Minimum day length limiting the PP response	
	SlaPente	Leaf Properties	none			Regression slope between SLA Max and Min	Between species
0.9955	AttenMitch	Leaf Properties	none	0.9955	ca. 0.9955	Mitscherlich coefficient function allowing a non-linear evolution of SLA from max to min	
1	TxAssimMatu1	Light Conversion and Extinction	fraction	1	0…1	Assimilation reduction factor during this phase	Only if there is terminal leaf senescence independent of competition
0.5	TxAssimMatu2	Light Conversion and Extinction	fraction	0.5	0…1	Assimilation reduction factor during this phase	Only if there is terminal leaf senescence independent of competition
1.5	CoefficientQ10	Maintenance Respiration	none	1.5	1…2	Q10 coefficient for maintenance respiration. No effect for value of 1, literature suggests a value of 2 when T° increases by 10°. A rate of 1.5 is suggested in recent literature	
1.2	KcMax	Water Related	fraction	1.2	1…1.5	FAO reference coefficient for	Between species, but adhere to

Default	Crop Parameters	Functional Group	Unit	Default	Value Range	Description	Used for
						vegetation cover evapotranspiration (ET) as a fraction of potential evapotranspiration (ETP)	FAO recommendations or observations
0.5	PFactor	Water Related	none	0.5	0…0.7	FAO reference for critical value FTSW of transpiration response. Value 0 = stomata respond immediately if FTSW<1. Most crops are around 0.5: response begins when half of available water is depleted. Rice is sensitive (value between 0.1 and 0.4)	Between species, but adhere to FAO recommendations or observations

B. Soil Parameters

Default	Soil and Plot Parameters	Functional Group	Unit	Default	Value Range	Description	Measurements
	StockIniSurf	Surface reservoir	mm		0…20	Initial water stock of the surface reservoir defined on the 1st simulation date corresponding to the measurement date.	
	StockIniProf	Depth reservoir	mm		0…100	Initial water stock of the depth reservoir defined on the 1st simulation date corresponding to the measurement date.	
	EpaisseurSurf	Surface reservoir	mm	200	50…200	Thickness of the surface reservoir	
	EpaisseurProf	Depth reservoir	mm		200…2000	Thickness of the depth reservoir, depends on the soil (root blockage by compacted soil) and the maximum rooting depth of the crop: 200 irrigated rice, 600 rainfed rice, 1200 maize & sorghum, 2000 millet…	
	PourcRuiss	Soil Typology	%			Percentage of water runoff beyond the runoff threshold (SeuiRuis) depending on rainfall amounts	
	SeuilRuiss	Soil Typology	mm			Daily rainfall threshold triggering runoff	
	RU	Soil Typology	mm/m			Deduced from HumCR (= HumFC) and HumPF	
	HumCR	Soil Typology	m^3/m^3			Volumetric soil moisture content at field capacity (water remaining after drainage following excessive irrigation, in the absence of evaporation)	

Default	Soil and Plot Parameters	Functional Group	Unit	Default	Value Range	Description	Measurements
	HumPF	Soil Typology	m³/m³	0.05	0.01…0.08	Volumetric soil moisture content at wilting point (root extraction power limit)	Measure by allowing a plant to extract water from the soil in a pot until the plant wilts, while perfectly preventing evaporation from the soil surface. Then measure the water content.
	HumFC	Soil Typology	m³/m³	0.25	0.1…0.3	Volumetric soil moisture content at field capacity (water remaining after drainage following excessive irrigation, in the absence of evaporation)	Measure by fully saturating the soil, then drain the pot until no more water flows from the drainage holes. Then measure the water content.
	HumSat	Soil Typology	m³/m³	0.35	0.2…0.5	Volumetric soil moisture content when completely filled with water, all air spaces being filled with water.	Measure by saturating the soil completely without compacting it. Difficult because gas can be trapped in the soil. Then measure the water content.
	PercolationMax	Soil Typology	mm	5	0…20	Daily percolation rate (deep drainage)	Measure by placing open-bottom lysimeters in the field, fill with water and cover against evaporation. Observe the decrease in the stagnant water column per day.

C. Practical Cultural Parameters

Default	Farming Practices	Functional Group	Unit	Default	Value Range	Description
	DatesSemis	dd/mm/yyyy	none	none		Observed sowing date or automatically researched sowing date (conditions allowing emergence and plant survival)
50	ProfRacIni	mm	50	5…100	Initial root depth (not used), transplantation case	
	Densite	plants/ha				Seeding density
	SeuilEauSemis	mm	10			Soil water threshold allowing germination
	NbjTestSemis	days	20			Mortality testing days (juvenile period)
	IrrigAuto	binary		0 or 1		If equal to 1, this allows simulating irrigation doses
0.6	IrrigAutoTarget	fraction (0…1)	0.6	0…1	Fraction of soil water stock triggering irrigation. E.g., if 0.6 irrigation will be triggered if we have a water stock below this threshold.	
	MaxIrrig	mm		5…70	Maximum irrigation water stock	
	Precision	mm		1..20	Precision of the calculations of the quantity to be irrigated (e.g., 5 corresponds to precision in 5 mm increments)	